

Kondo temperature of Anderson impurity model in a quantum wire with spin-orbit coupling

Liang Chen^{1,*} and Rong-Sheng Han^{1,†}

¹*Mathematics and Physics Department, North China Electric Power University, Beijing, 102206, China*
(Dated: September 14, 2021)

We use two different methods, the Hirsch-Fye quantum Monte Carlo simulation and the slave-boson mean field analysis to estimate the effect of spin-orbit coupling on the Kondo temperature in a quantum wire. In quantum Monte Carlo simulation, we calculate the product of spin susceptibility and temperature for different spin-orbit couplings and impurity energies. The variation of the Kondo temperature is estimated via the low temperature universal curves. In the mean field analysis, the Kondo temperature is estimated as the condensation temperature of slave-boson. Both the two methods demonstrate that the Kondo temperature is almost a linear function of the spin-orbit energy, and that the Kondo temperature is suppressed by the spin-orbit coupling. Our results are dramatically different from those given by the perturbative renormalization group analysis.

PACS numbers: 72.10.Fk, 71.70.Ej, 72.15.Qm

I. INTRODUCTION

Spin-orbit coupling¹ (SOC), the interaction between a quantum particle's spin and the effective magnetic field induced by its (orbital) motion, has attracted much attention as an useful tool for the realization of spintronics in the last few decades²⁻⁴. In recent years, SOC plays an important role in the topological nontrivial quantum materials, e.g., topological insulator^{5,6}, topological superconductor⁷, quantum anomalous Hall effect⁸, Weyl semimetal⁹, Majorana fermion^{10,11}, etc. Magnetic doping in these systems is an efficient method to tune and control the transport properties for some of these systems, e.g. breaking the time-reversal symmetry and inducing a finite band gap on the surface of topological insulator.

The Kondo effect in some of these SOC systems has been theoretically investigated¹² and experimentally confirmed¹³. However, as a fundamental problem, the effect of SOC on the Kondo temperature is still unclear as far as we know. In recent years, several theoretical works have investigated this problem¹⁴⁻²⁰. By studying the standard Kondo model in a two-dimensional electron gas, Malecki¹⁴ conclude that the Kondo effect is robust against Rashba SOC. However, it is demonstrated^{15,21} that the standard Kondo model in SOC systems is incomplete. Under a generalized Schrieffer-Wolff transformation of the Anderson impurity model in two-dimensional electron gas with Rashba SOC, Zarea et al.¹⁵ find that, in addition to the usual Kondo interaction, there is another Dzyaloshinskii-Moriya interaction between the magnetic impurity and the conduction electrons. Using the perturbative renormalization group analysis, they conclude that the Kondo temperature is exponentially enhanced by the SOC. However, both the numerical renormalization group calculation^{16,18} and the quantum Monte Carlo simulation²⁰ show that the Kondo temperature is almost a linear function of the spin-orbit energy.

Recently, Sousa et al.²¹ find that the effect of SOC

on the Kondo temperature in the one-dimensional quantum wire is special due to the discontinuity of the fermi surface. In addition to the traditional spin-flipping scattering and the Dzyaloshinskii-Moriya interaction in SOC system, there is another process for one-dimensional quantum wire, the Elliott-Yafet scattering. The combination of these two processes, Dzyaloshinskii-Moriya interaction and Elliott-Yafet scattering, makes the Kondo temperature exponentially enhanced by the SOC. However, these conclusions are based on the perturbative renormalization group analysis, a non-perturbation study is still opening. In this paper, we use the Hirsch-Fye quantum Monte Carlo (HFQMC) simulation and the slave-boson mean field theory (SBMF) to study the single-impurity Anderson model in quantum wire with both Rashba and linear Dresselhaus SOC, and estimate the effect of the SOC on the Kondo temperature.

The rest of the paper is organized as follows. We present the Anderson impurity model in Sec. II. The HFQMC simulations are given in Sec. III. Sec. IV presents the formulation and results of the SBFM analysis. A discussion is given in Sec. V.

II. MODEL HAMILTONIAN

The single-impurity Anderson model in quantum wire with Rashba and linear Dresselhaus SOC is formulated as, $H = H_{\text{wire}} + H_{\text{dot}} + H_{\text{hyb}}$, where,

$$H_{\text{dot}} = \sum_{s=\uparrow,\downarrow} \varepsilon_d n_s + U n_{\uparrow} n_{\downarrow}, \quad (1)$$

describes the quantum impurity, in which $s = \uparrow, \downarrow$ refer to the spin-up and spin-down impurity states, $n_s = d_s^\dagger d_s$ is the occupation number of spin-s state, d_s^\dagger and d_s are the creation and annihilation operators of the spin-s impurity state, respectively. U is the Hubbard interaction between the occupied spin-up and spin-down states on the impurity energy level ε_d . The Hamiltonian of the

quantum wire is given by,

$$H_{\text{wire}} = \sum_{k,ss'} [\varepsilon_k + k(\gamma_D \sigma_{ss'}^x - \gamma_R \sigma_{ss'}^y)] c_{ks}^\dagger c_{ks'}, \quad (2)$$

where k is the wave-vector of the conduction electron state along the z axis, $\varepsilon_k = \hbar^2 k^2 / 2m^* - E_F$ is the kinetic energy represented with effective mass m^* . E_F is the Fermi energy. γ_R and γ_D are the Rashba and the linear Dresselhaus SOC. $\sigma^{(x,y)}$ are the first two Pauli matrices. c_{ks}^\dagger and c_{ks} are the creation and annihilation operators of the electron state with wave-vector k and spin s . The hybridization between the isolated impurity and the quantum wire is represented as,

$$H_{\text{hyb}} = \sum_{ks} \left(V_k c_{ks}^\dagger d_s + V_k^* d_s^\dagger c_{ks} \right), \quad (3)$$

where V_k is the hybridization matrix element. Without loss of generality, we assume that the hybridization is short ranged, so that V_k is wave-vector independent, $V_k = V$.

The conduction band electron states in the quantum wire can be integrated out to get the partition function of the impurity states,

$$\mathcal{Z} = \int \mathcal{D}d_s^\dagger \mathcal{D}d_s e^{-\mathcal{S}}, \quad (4)$$

$$\mathcal{S} = \int_0^\beta d\tau \left[d_s^\dagger \left(\frac{\partial}{\partial \tau} + \varepsilon_d + \Sigma_d \right) d_s + U d_\uparrow^\dagger d_\uparrow d_\downarrow^\dagger d_\downarrow \right], \quad (5)$$

where $\beta = 1/k_B T$ is the inverse temperature, k_B is the Boltzmann constant. The effect of the conduction band electron states is included in the self-energy of the impurity states, Σ_d . In the imaginary-frequency representation, the self-energy is given in the following form,

$$\Sigma_d(i\omega_n) = -\frac{i \Gamma \operatorname{sgn}[\operatorname{Im}(i\omega)]}{\sqrt{2(i\omega_n + E_F) + E_\gamma}}, \quad (6)$$

where $\Gamma = \rho V^2$ is the hybridization strength in the conventional form, ρ is the density of states (DOS). $\omega_n = (2n+1)\pi k_B T$ is the Matsubara frequency of Fermion. It is easy to check that, the total DOS of the non-interacting quantum wire, $\rho(\varepsilon) = \rho_\uparrow(\varepsilon) + \rho_\downarrow(\varepsilon)$, is proportional to the imaginary part of $\Sigma_d(\varepsilon + i0^+)$. In the non-interacting limit, $U \rightarrow 0$, the imaginary-time free Green's function of the impurity state is given by the Fourier transformation,

$$G_0(\tau) = \frac{1}{\beta} \sum_n e^{-i\omega_n \tau} [i\omega_n + E_F - \varepsilon_d - \Sigma(i\omega_n)]^{-1}. \quad (7)$$

Once we get the imaginary-time free Green's function, we can use the HFQMC method to solve the magnetic impurity problem.

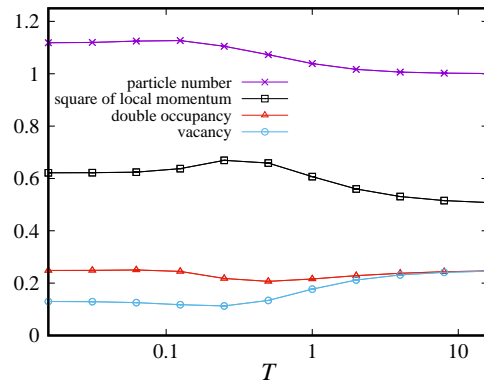


FIG. 1. (color online) The particle number $n = n_\uparrow + n_\downarrow$, square of local moment, $m^2 = (n_\uparrow - n_\downarrow)^2$, vacancy $(1 - n_\uparrow)(1 - n_\downarrow)$, and double occupancy (with error-bars) vs temperature. Parameters used in the simulation: hybridization $\Gamma = 0.05\pi$, Fermi energy $E_F = 0.2$, impurity energy level $\varepsilon_d = -0.5$, Hubbard interaction $U = 1$, spin-orbit energy $E_\gamma = 0$.

III. HIRSCH-FYE QUANTUM MONTE CARLO SIMULATION

In the HFQMC calculation, the Hubbard interaction is simulated by the statistical average over the auxiliary Ising pseudo-spin configurations. In the following numerical simulations, all of the results are averaged over 20 independent samples, and every sample runs over 2000 HFQMC loops after warm-up. HFQMC is numerical non-perturbative method, it is widely used in the previous works, i.e. the local moment of magnetic impurity^{22,23}, the competition between Kondo screen and Ruderman-Kittel-Kasuya-Yosida (RKKY) interaction for two-impurity Anderson model^{24,25}, the local moment formation in dilute magnetic semiconductors²⁶ and graphene²⁷, the RKKY interaction in a topological insulator²⁸.

Fig 1 shows four important static physical quantities, the particle number $n = n_\uparrow + n_\downarrow$, the square of local moment $m^2 = (n_\uparrow - n_\downarrow)^2$, the vacancy $(1 - n_\uparrow)(1 - n_\downarrow)$, and the double occupancy $n_\uparrow n_\downarrow$ vs temperature. From this plotting, we find three results. Firstly, the particle number $n = n_\uparrow + n_\downarrow \approx 1$, which demonstrates that the Hubbard interaction $U = 1$ is strong enough for the formation of local moment states. Secondly, the square of local moment, $m^2 = (n_\uparrow - n_\downarrow)^2$, has a maximum point at the intermedia region, $0.1 < T < 1$, which demonstrates that the local moment is formed in this region and further screened in the strong correlation region, $T < 0.1$. Thirdly, the statistical error bars are plotted and most of them are too small to be observed, which demonstrates that 20 samples and 2000 loops for each sample are accurate enough for this problem.

Now we consider the effect of SOC on the Kondo temperature. This situation has been studied in Ref. [21] by using the perturbative renormalization group method. Here we use the universal curve to study the problem. In

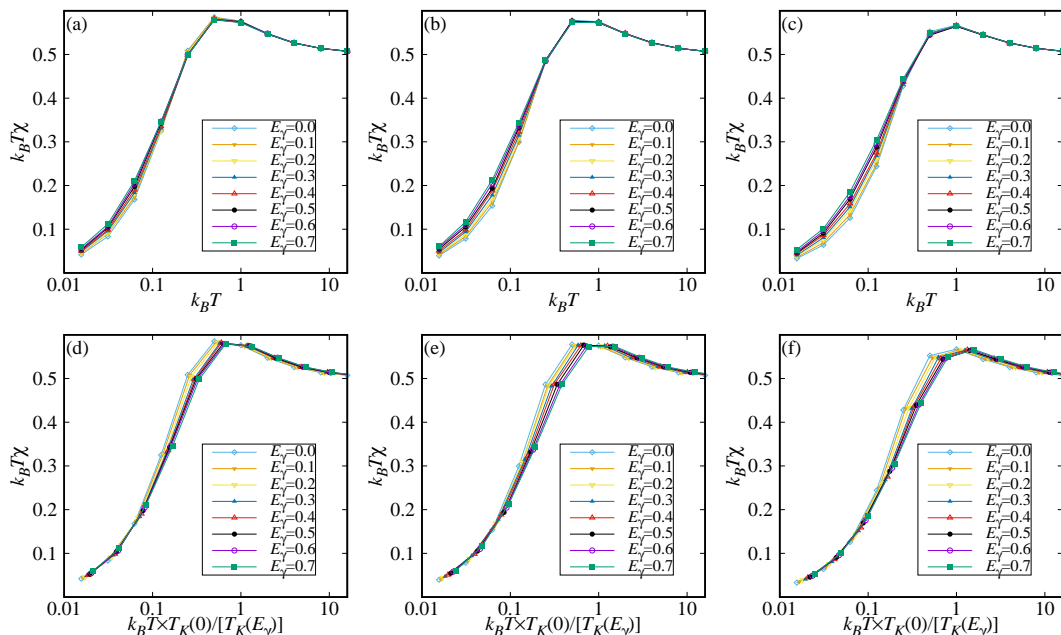


FIG. 2. (color online) (a)-(c), the product $k_B T \chi$ vs temperature for different impurity energies, spin-orbit energies: (a) $\varepsilon_d = -0.3$, (b) $\varepsilon_d = -0.5$, (c) $\varepsilon_d = -0.7$. (d)-(f) the product $k_B T \chi$ vs rescaled temperatures corresponding to (a)-(c), respectively. Model parameters used in these simulations: $\Gamma = 0.05\pi$, $U = 1.0$, $E_F = 0.2$, $h = 0$.

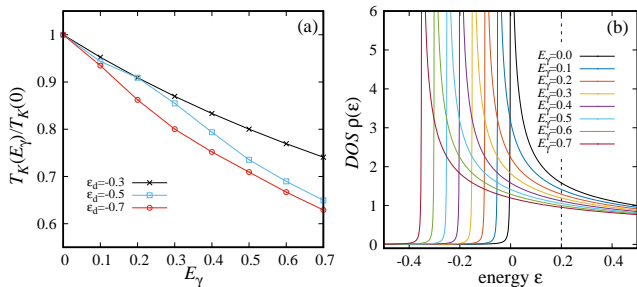


FIG. 3. (color online) (a) The variation of Kondo temperature T_K vs spin-orbit energy E_γ for three different impurity energies $\varepsilon = -0.3, -0.5, -0.7$, fitted from Fig. 2. (b) The DOS for different spin-orbit energies from $E_\gamma = 0$ to $E_\gamma = 0.7$.

the seminal paper [29], the Kondo temperature is related to the product of temperature and impurity spin susceptibility via the following universal relationship,

$$\Phi[4k_B T \chi(T) - 1] = \ln(T/T_K), \quad (8)$$

where Φ is a universal function and the impurity spin susceptibility $\chi(T)$ is defined as,

$$\chi(T) = \int_0^\beta d\tau \langle S_z(\tau) S_z(0) \rangle, \quad (9)$$

$S_z(\tau) = [n_\uparrow(\tau) - n_\downarrow(\tau)]/2$. Fig. 2 (a)-(c) show the product of temperature and spin susceptibility vs temperature for different parameters. According to Eq. (8), we keep the Y-axis unchanged and the X-axis rescaled, such that

in the low temperature region ($k_B T < 0.1$) the curves coincide to each other. The results are plotted in Fig. 2 (d)-(f). The rescaling defines the variation of the Kondo temperature $T_K(E_\gamma)/T_K(0)$ vs the spin-orbit energy, as shown in Fig. 3(a). One can find that (a) the Kondo temperature T_K is almost a linear function of the spin-orbit energy E_γ , (b) the Kondo temperature is suppressed by the spin-orbit energy. This is qualitatively different from those given by the perturbative renormalization group theory, which show that the Kondo temperature is exponentially enhanced by the spin-orbit energy. Qualitatively, this is easy to understand. Fig. 3(b) shows the DOS for different spin-orbit energies. One can find that, the larger spin-orbit energy will induce a smaller DOS on the Fermi surface, $E_F = 0.2$, which demonstrates that a lower Kondo temperature is required to screen the local moment state. For the model (1)-(3), our non-perturbative simulations show that the variation of the Kondo temperature is dominated by the alternation of the DOS on the Fermi surface, rather than the Dzyaloshinskii-Moriya interaction or Elliott-Yafet spin-flip scattering mechanism proposed in Ref. [21].

IV. SLAVE-BOSON MEAN FIELD ANALYSIS

In order to be more persuasive, we use another approach, the SBMF method, to estimate the effect of the SOC on the Kondo temperature. SBMF is used in the previous studies of the Anderson impurity in the mixed-valence regime^{30,31}, the Anderson lattice model³²⁻³⁴, and

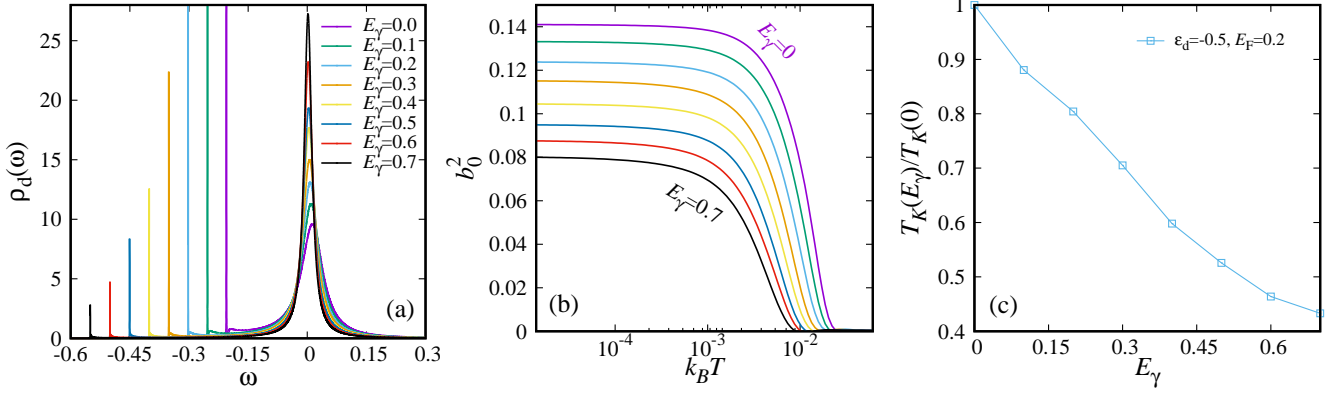


FIG. 4. (color online) (a) The density of states of the impurity for different spin-orbit energies from $E_\gamma = 0$ to $E_\gamma = 0.7$. (b) b_0^2 vs temperature for different spin-orbit energies. (c) The variation of the Kondo temperature vs spin-orbit energy estimated from the vanishing point of b_0^2 . The other parameters are chosen as $E_F = 0.2$, $\Gamma = 0.05\pi$.

the low-energy physics in strong correlation systems such as the magnetic impurity resonance states in a d -wave superconductor³⁵ and iron-based superconductors³⁶. We consider a strong on-site Coulomb interaction on the impurity, $U \rightarrow \infty$. In this limit, only the empty state and the singly occupied states are allowed. An auxiliary boson field, is introduced to reformulate the annihilation and creation operators of the impurity state as,

$$d_s = b^\dagger f_s, \quad d_s^\dagger = f_s^\dagger b, \quad (10)$$

where b^\dagger and b are the boson creation and annihilation operators of the empty states, f_s^\dagger and f_s are the fermion operators of the singly occupied states. These states expand the whole Hilbert space of the impurity with strong Coulomb interaction, such that these operators have to obey the local constraint $b^\dagger b + \sum_s f_s^\dagger f_s = 1$. Under the mean field approximation, the local constraint is approximated by adding a term $\lambda_0(b^\dagger b + \sum_s f_s^\dagger f_s - 1)$ to the model Hamiltonian, where λ_0 is a Lagrangian multiplier. The boson operators, b and b^\dagger are approximated by a complex number b_0 and its complex conjugate b_0^* . Without loss of generality, here we assume that b_0 is a real number. Substituting Eq. (10) in to Eq. (1) and Eq. (3), we get,

$$H_{\text{dot}} = \sum_s \tilde{\epsilon}_d f_s^\dagger f_s + \lambda_0(b_0^2 - 1), \quad (11)$$

$$H_{\text{hyb}} = \sum_{k,s} \left(\tilde{V}_k c_{k,s}^\dagger f_s + \tilde{V}_k^* f_s^\dagger c_{k,s} \right), \quad (12)$$

in the SBMF approximation, where $\tilde{\epsilon}_d = \epsilon_d + \lambda_0$ is the renormalized impurity energy and $\tilde{V}_k = b_0 V_k$ is the renormalized hybridization strength. Following the procedure presented in Sec. III, we can finish the integration over the fermion states and get the partition function,

$$\mathcal{Z} = \exp \left\{ \beta \lambda_0 (1 - b_0^2) + 2 \sum_n \log \left[i\omega_n - \tilde{\epsilon}_d - \tilde{\Sigma}_d(i\omega_n) \right] \right\}. \quad (13)$$

The free energy is given by,

$$\begin{aligned} \mathcal{F} &= -\frac{1}{\beta} \log(\mathcal{Z}) \\ &= \lambda_0(b_0^2 - 1) - \frac{2}{\beta} \sum_n \log \left[i\omega_n - \tilde{\epsilon}_d - \tilde{\Sigma}(i\omega_n) \right], \end{aligned} \quad (14)$$

where the renormalized self energy is,

$$\tilde{\Sigma}(i\omega_n) = -\frac{i \tilde{\Gamma} \operatorname{sgn}[\operatorname{Im}(i\omega_n)]}{\sqrt{2(i\omega_n + E_F) + E_\gamma}}, \quad \tilde{\Gamma} = b_0^2 \Gamma. \quad (15)$$

The parameters λ_0 and b_0^2 are determined by minimizing the free energy \mathcal{F} . We get the following expressions,

$$\frac{2}{\beta} \sum_n \frac{1}{i\omega_n - \tilde{\epsilon}_d - \tilde{\Sigma}(i\omega_n)} + b_0^2 - 1 = 0, \quad (16)$$

$$\frac{2}{\beta} \sum_n \frac{\tilde{\Sigma}(i\omega_n)}{i\omega_n - \tilde{\epsilon}_d - \tilde{\Sigma}(i\omega_n)} + \lambda_0 b_0^2 = 0. \quad (17)$$

Taking the analytical continuation, $i\omega_n \rightarrow \omega + i0^+$, we can rewrite these expressions in the real-frequency formalism,

$$2 \int_{-\infty}^{\infty} d\omega \frac{\rho_d(\omega)}{e^{\beta\omega} + 1} + b_0^2 - 1 = 0, \quad (18)$$

$$2 \int_{-\infty}^{\infty} d\omega \frac{(\omega - \tilde{\epsilon}_d) \rho_d(\omega)}{e^{\beta\omega} + 1} + \lambda_0 b_0^2 = 0. \quad (19)$$

where $\rho_d(\omega)$ is the density of impurity states,

$$\rho_d(\omega) = -\frac{1}{\pi} \frac{\operatorname{Im} \tilde{\Sigma}(\omega)}{[\omega - \tilde{\epsilon}_d - \operatorname{Re} \tilde{\Sigma}(\omega)]^2 + [\operatorname{Im} \tilde{\Sigma}(\omega)]^2}, \quad (20)$$

$\tilde{\Sigma}(\omega)$ is the analytical continuation of $\tilde{\Sigma}(i\omega_n)$, its explicit expression is given by,

$$\operatorname{Re} \tilde{\Sigma}(\omega) = -\frac{\tilde{\Gamma} \Theta(-\omega - E_F - \frac{1}{2} E_\gamma)}{\sqrt{2(\omega + E_F) + E_\gamma}}, \quad (21)$$

$$\operatorname{Im} \tilde{\Sigma}(\omega) = -\frac{\tilde{\Gamma} \Theta(\omega + E_F + \frac{1}{2} E_\gamma)}{\sqrt{2(\omega + E_F) + E_\gamma}}, \quad (22)$$

where $\Theta(x)$ is the step function. The Kondo temperature T_K is estimated as the T that makes the slave-boson parameter b_0^2 vanishing^{33,34}, the condensation temperature of the slave-boson.

It is difficult to get the analytical solution of Eqs. (18)-(19), here we show the numerical results. Unless otherwise noted, in the following calculations we choose the Fermi energy $E_F = 0.2$, impurity energy $\varepsilon_d = -0.5$, and hybridization strength $\Gamma = 0.05\pi$. Fig. 4(a) shows the zero-temperature density of states of the impurity, $\rho_d(\omega)$, calculated using the SBMF method. We find that, in addition to the Kondo resonance peak near the Fermi surface ($\omega = 0$), there is another sharp peak. This additional peak is induced by the divergence of the density of states at the conduction band edge. One can find that, when the spin-orbit energy increases from $E_\gamma = 0$ to $E_\gamma = 0.7$, the sharp peak come from the conduction band edge is dramatically decreased. Meanwhile, the Kondo resonance peak gets more sharp, which demonstrates that the Kondo temperature is suppressed by the SOC. In order to get a more quantitative result, Fig. 4(b) shows b_0^2 as a function of the temperature T for several values of spin-orbit energies varying from $E_\gamma = 0$ to $E_\gamma = 0.7$. We find that b_0^2 is vanishing in the temperature region 0.01 to 0.1, and the Kondo temperature, T_K , which is defined as the condensation temperature where $b_0^2 = 0$, is suppressed by the spin-orbit energy. Quantitatively, Fig. 4(c) shows the variation of T_K vs spin-orbit energy E_γ . One can find that the Kondo temperature is almost a linear function of the spin-orbit energy, and that T_K is suppressed by the SOC. These results are consistent with the estimation from the HFQMC simulations.

V. DISCUSSION

In this paper, we use two different methods, the unbiased HFQMC simulation and the SBMF analysis to

study the effect of SOC on the Kondo temperature in a quantum wire. Both the two methods show that the Kondo temperature is suppressed by the SOC, and that the Kondo temperature is almost a linear function of the spin-orbit energy. Our results are qualitatively different from the perturbative renormalization group analysis. In the perturbative renormalization group analysis, the Kondo temperature is always enhanced by the SOC, and an exponential enhancement is predicted.

For the linear dependence of T_K on the spin-orbit coupling, our results are consistent with Refs. [16] and [20]. However, both Refs. [16] and [20] show that the T_K can be enhanced or depressed by SOC in the two-dimensional electron gas system. For the one-dimensional quantum wire, we find that the Kondo temperature is always suppressed by SOC. This distinction comes from the explicit difference of the form of DOS in the two-dimensional electron gas and the one-dimensional quantum wire. For the two-dimensional electron gas, as shown in [16] and [20], the DOS on the Fermi surface is invariant for different SOC's if $E_F > 0$. Which makes the details of ε_d , U , and Γ being important, and the Kondo temperature being either enhanced or suppressed by SOC. However, for the one-dimensional quantum wire, the DOS on the Fermi surface is variable for different E_γ 's. Further more, one can find from Fig. 3(b) that the DOS on the Fermi surface is a decreasing function of E_γ . This influence dominates that the Kondo temperature is suppressed by the SOC.

ACKNOWLEDGMENT

LC would like to express his gratitude to Prof. H.-Q. Lin, J. Sun, and H.-K. Tang for the original HFQMC code. We appreciate the support from the NSFC under Grant Nos. 11504106 and 11447167 and the Fundamental Research Funds for the Central Universities.

* Corresponding Email: slchern@ncepu.edu.cn

† Corresponding Email: hqs@ncepu.edu.cn

¹ R. Winkler, *Spin-orbit Coupling Effects in Two-Dimensional Electron and Hole Systems* (Springer-Verlag, Berlin, Heidelberg, 2003).

² I. Žutić, J. Fabian, and S. Das Sarma, *Rev. Mod. Phys.* **76**, 323 (2004).

³ T. Koga, J. Nitta, T. Akazaki, and H. Takayanagi, *Phys. Rev. Lett.* **89**, 046801 (2002).

⁴ Z. Y. Zhu, Y. C. Cheng, and U. Schwingenschlögl, *Phys. Rev. B* **84**, 153402 (2011).

⁵ M. Z. Hasan and C. L. Kane, *Rev. Mod. Phys.* **82**, 3045 (2010).

⁶ X.-L. Qi and S.-C. Zhang, *Rev. Mod. Phys.* **83**, 1057 (2011).

⁷ R. M. Lutchyn, J. D. Sau, and S. Das Sarma, *Phys. Rev. Lett.* **105**, 077001 (2010).

⁸ C.-Z. Chang, J. Zhang, X. Feng, J. Shen, Z. Zhang, M. Guo, K. Li, Y. Ou, P. Wei, L.-L. Wang, Z.-Q. Ji, Y. Feng, S. Ji, X. Chen, J. Jia, X. Dai, Z. Fang, S.-C. Zhang, K. He, Y. Wang, L. Lu, X.-C. Ma, and Q.-K. Xue, *Science* **340**, 167 (2013).

⁹ X. Wan, A. M. Turner, A. Vishwanath, and S. Y. Savrasov, *Phys. Rev. B* **83**, 205101 (2011).

¹⁰ V. Mourik, K. Zuo, S. M. Frolov, S. R. Plissard, E. P. A. M. Bakkers, and L. P. Kouwenhoven, *Science* **336**, 1003 (2012).

¹¹ A. Das, Y. Ronen, Y. Most, Y. Oreg, M. Heiblum, and H. Shtrikman, *Nat Phys* **8**, 887 (2012).

¹² H.-F. Lü, H.-Z. Lu, S.-Q. Shen, and T.-K. Ng, *Phys. Rev. B* **87**, 195122 (2013).

¹³ J. J. Cha, J. R. Williams, D. Kong, S. Meister, H. Peng, A. J. Bestwick, P. Gallagher, D. Goldhaber-Gordon, and Y. Cui, *Nano Letters* **10**, 1076 (2010).

¹⁴ J. Malecki, *J. Stat. Phys.* **129**, 741 (2007).

- ¹⁵ M. Zarea, S. E. Ulloa, and N. Sandler, *Phys. Rev. Lett.* **108**, 046601 (2012).
- ¹⁶ R. Žitko and J. Bonča, *Phys. Rev. B* **84**, 193411 (2011).
- ¹⁷ L. Isaev, D. F. Agterberg, and I. Vekhter, *Phys. Rev. B* **85**, 081107 (2012).
- ¹⁸ A. Wong, S. E. Ulloa, N. Sandler, and K. Ingersent, *Phys. Rev. B* **93**, 075148 (2016).
- ¹⁹ A. Agarwala and V. B. Shenoy, *Phys. Rev. B* **93**, 241111 (2016).
- ²⁰ L. Chen, J. Sun, H.-K. Tang, and H.-Q. Lin, *J. Phys.: Condens. Matter* **28**, 396005 (2016).
- ²¹ G. R. de Sousa, J. F. Silva, and E. Vernek, *Phys. Rev. B* **94**, 125115 (2016).
- ²² J. E. Hirsch and R. M. Fye, *Phys. Rev. Lett.* **56**, 2521 (1986).
- ²³ R. M. Fye and J. E. Hirsch, *Phys. Rev. B* **38**, 433 (1988).
- ²⁴ R. M. Fye, J. E. Hirsch, and D. J. Scalapino, *Phys. Rev. B* **35**, 4901 (1987).
- ²⁵ R. M. Fye and J. E. Hirsch, *Phys. Rev. B* **40**, 4780 (1989).
- ²⁶ N. Bulut, K. Tanikawa, S. Takahashi, and S. Maekawa, *Phys. Rev. B* **76**, 045220 (2007).
- ²⁷ F. M. Hu, T. Ma, H.-Q. Lin, and J. E. Gubernatis, *Phys. Rev. B* **84**, 075414 (2011).
- ²⁸ J. Sun, L. Chen, and H.-Q. Lin, *Phys. Rev. B* **89**, 115101 (2014).
- ²⁹ H. R. Krishna-murthy, J. W. Wilkins, and K. G. Wilson, *Phys. Rev. B* **21**, 1003 (1980).
- ³⁰ P. Coleman, *Phys. Rev. B* **29**, 3035 (1984).
- ³¹ P. Coleman, *Phys. Rev. B* **35**, 5072 (1987).
- ³² V. Dorin and P. Schlottmann, *Phys. Rev. B* **47**, 5095 (1993).
- ³³ R. Franco, M. S. Figueira, and M. E. Foglio, *Phys. Rev. B* **66**, 045112 (2002).
- ³⁴ L. H. Nunes, M. Figueira, and M. Foglio, *Physics Letters A* **358**, 313 (2006).
- ³⁵ J.-X. Zhu and C. S. Ting, *Phys. Rev. B* **63**, 020506 (2000).
- ³⁶ A. Akbari, I. Eremin, and P. Thalmeier, *Phys. Rev. B* **81**, 014524 (2010).